

Plate 4. Elements of the scattering matrix vs scattering angle and effective size parameter for polydisperse spheres.

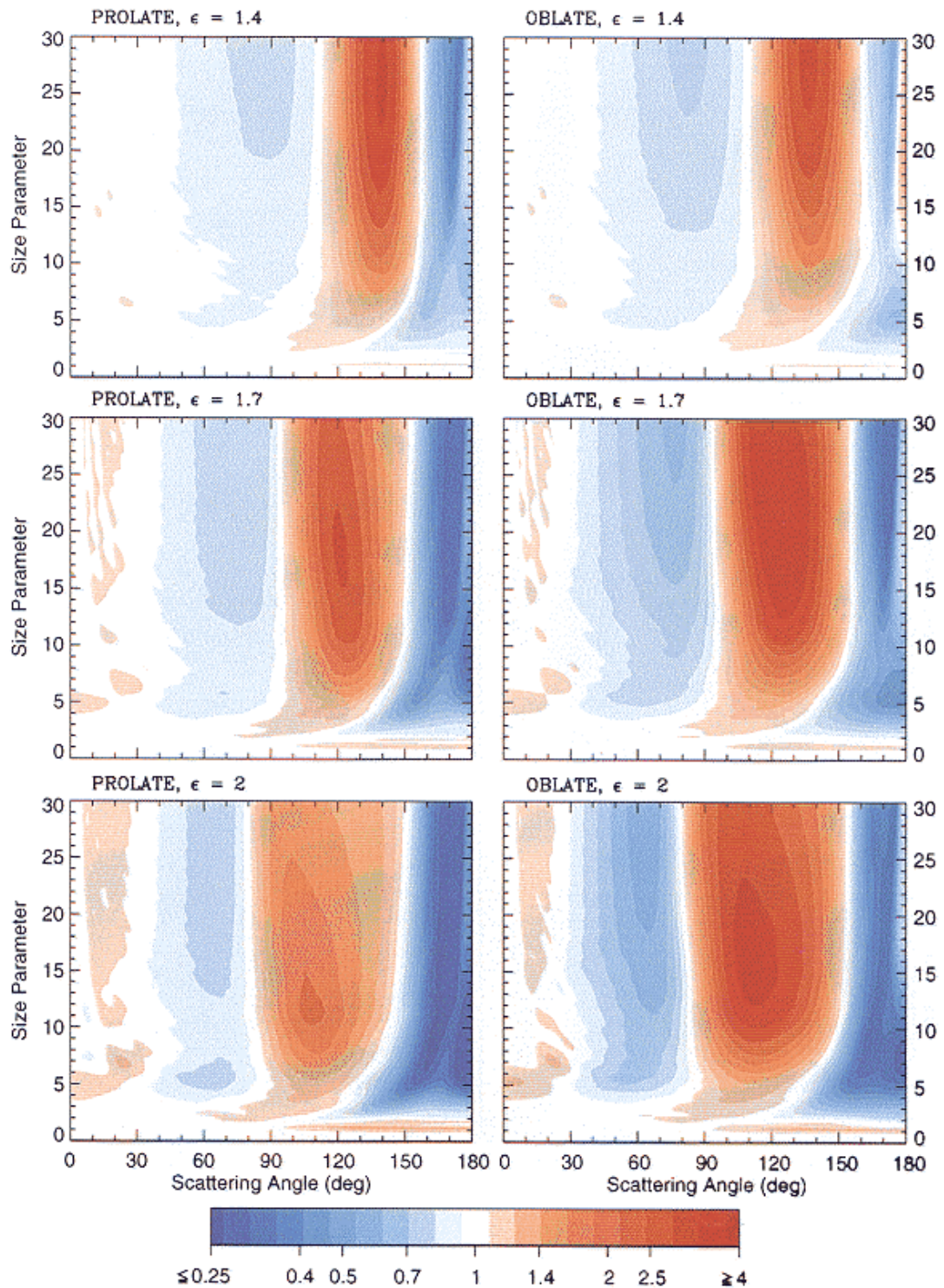


Plate 5. Ratio of the phase function for randomly oriented polydisperse spheroids to that for surface equivalent spheres vs scattering angle and effective size parameter.

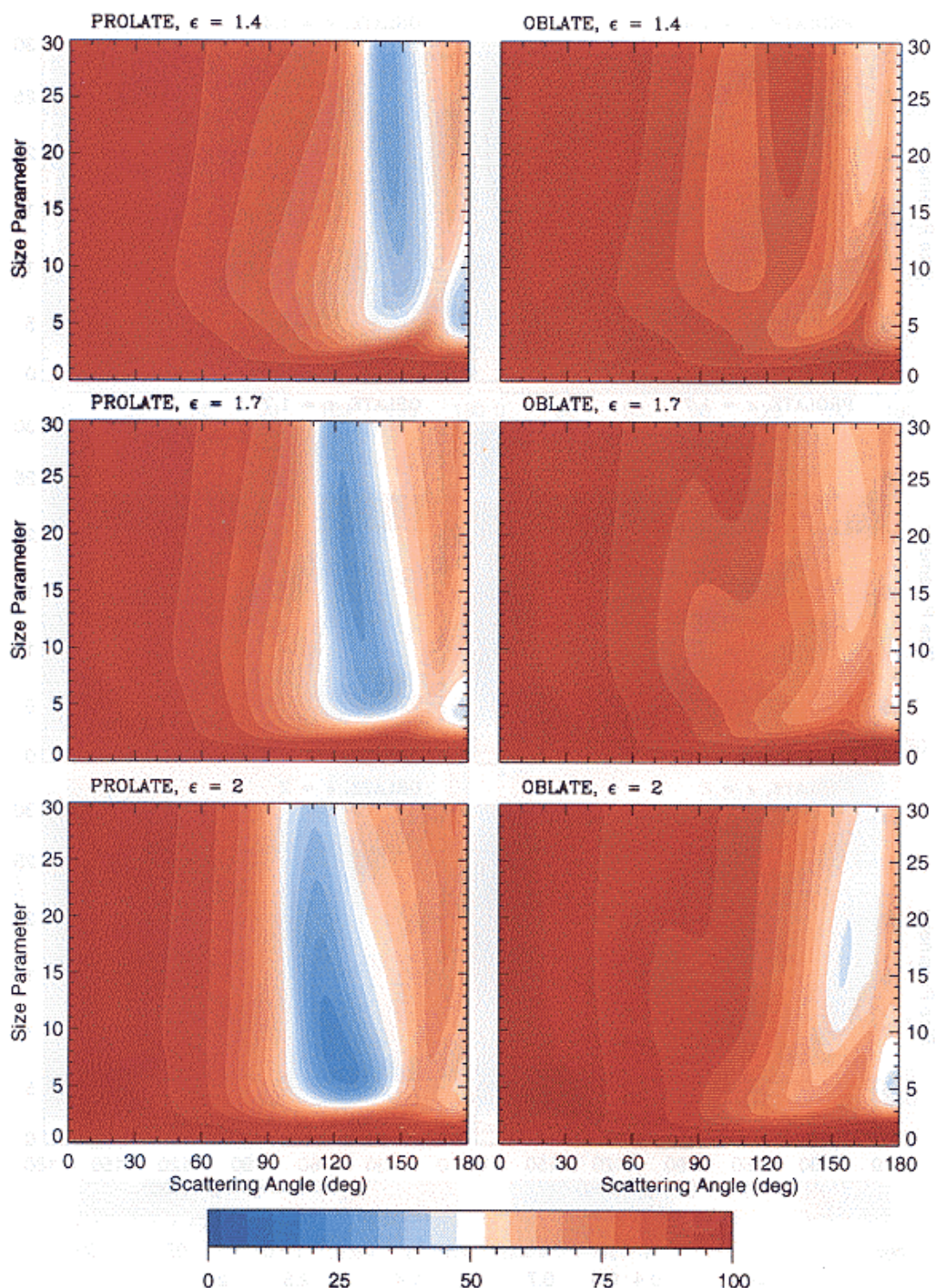


Plate 6. Ratio F_{22}/F_{11} in % vs scattering angle and effective size parameter for randomly oriented polydisperse spheroids.

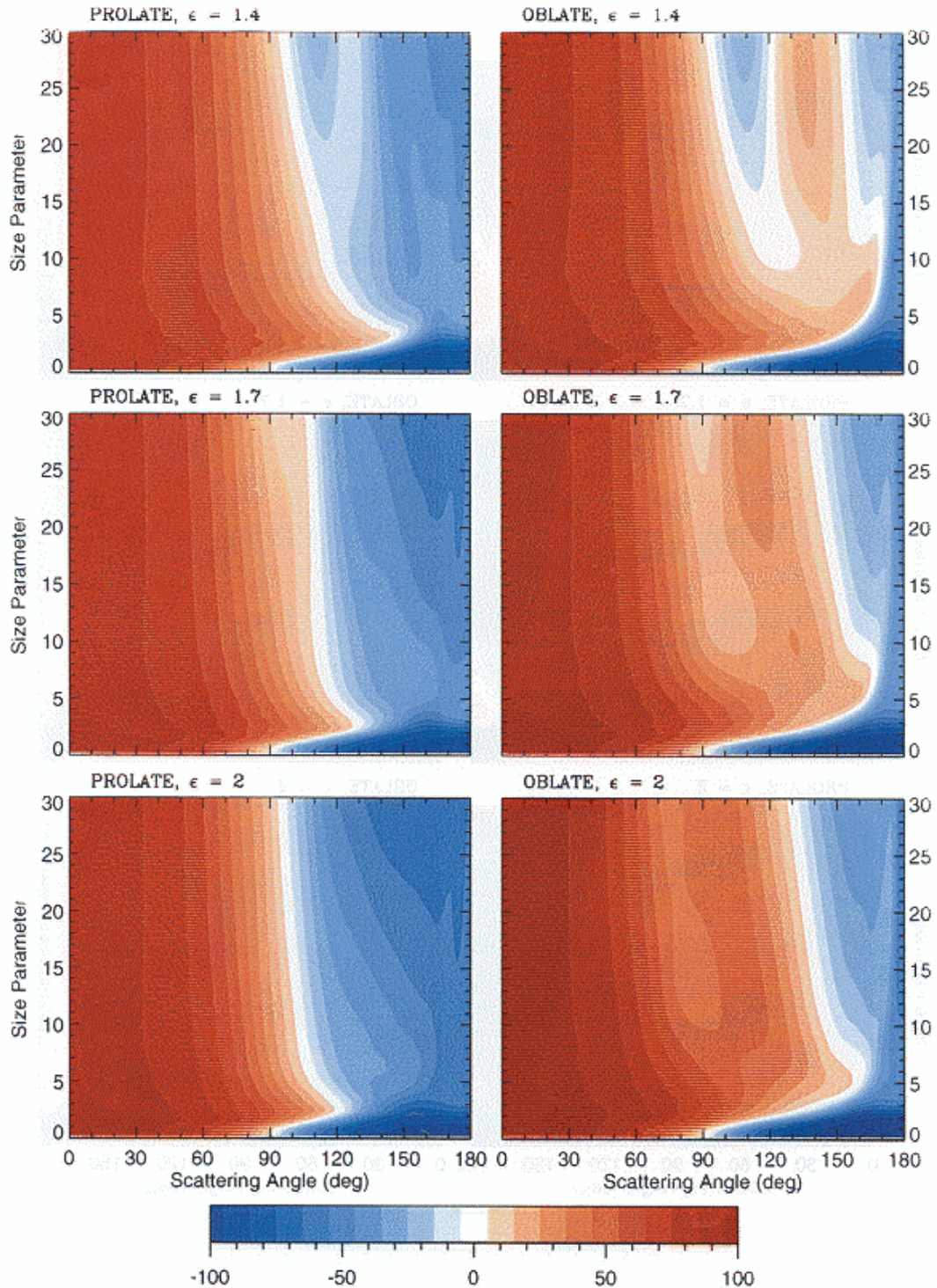


Plate 7. Ratio F_{33}/F_{11} in % vs scattering angle and effective size parameter for randomly oriented polydisperse spheroids.

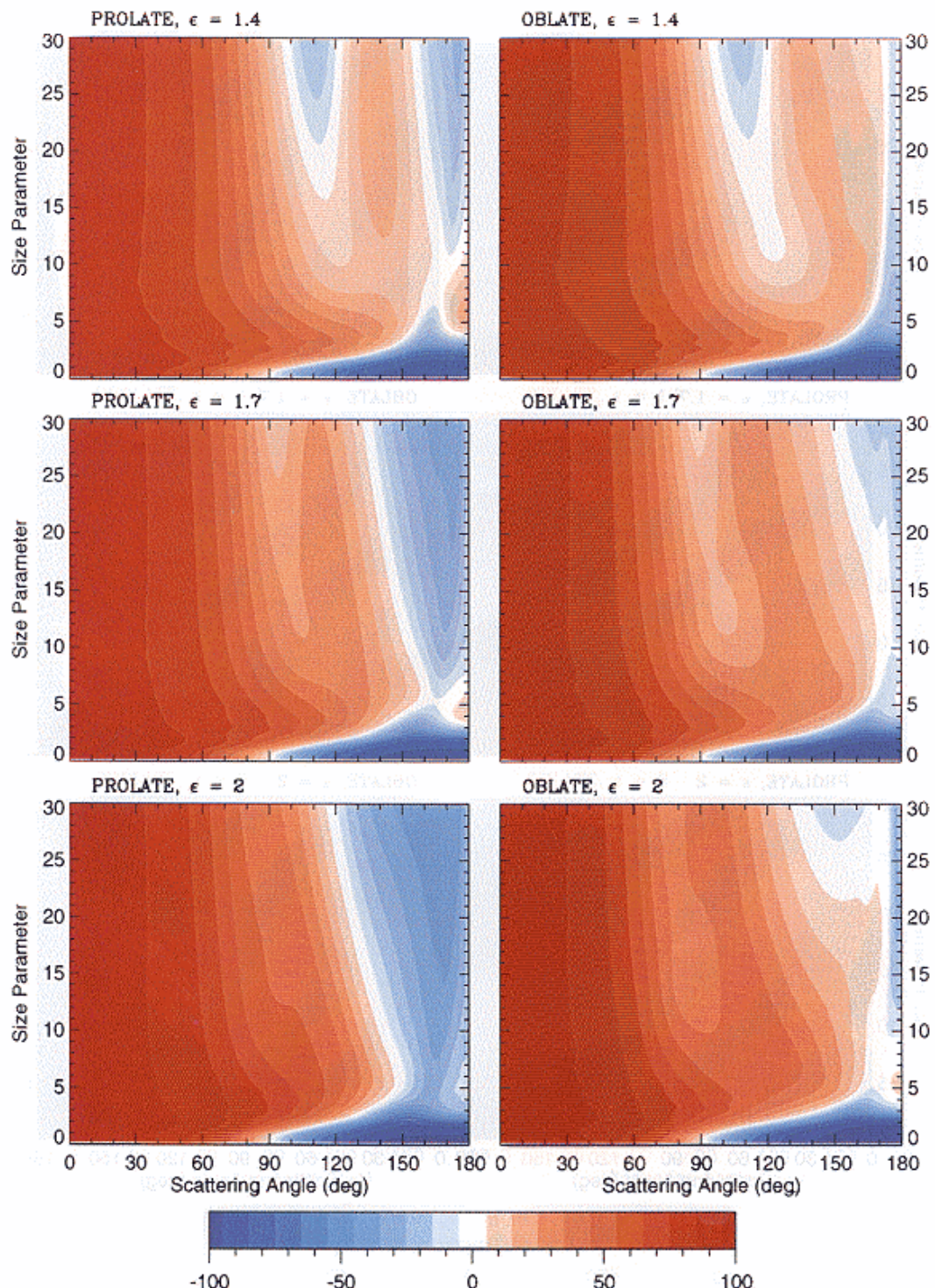


Plate 8. Ratio F_{44}/F_{11} in % vs scattering angle and effective size parameter for randomly oriented polydisperse spheroids.

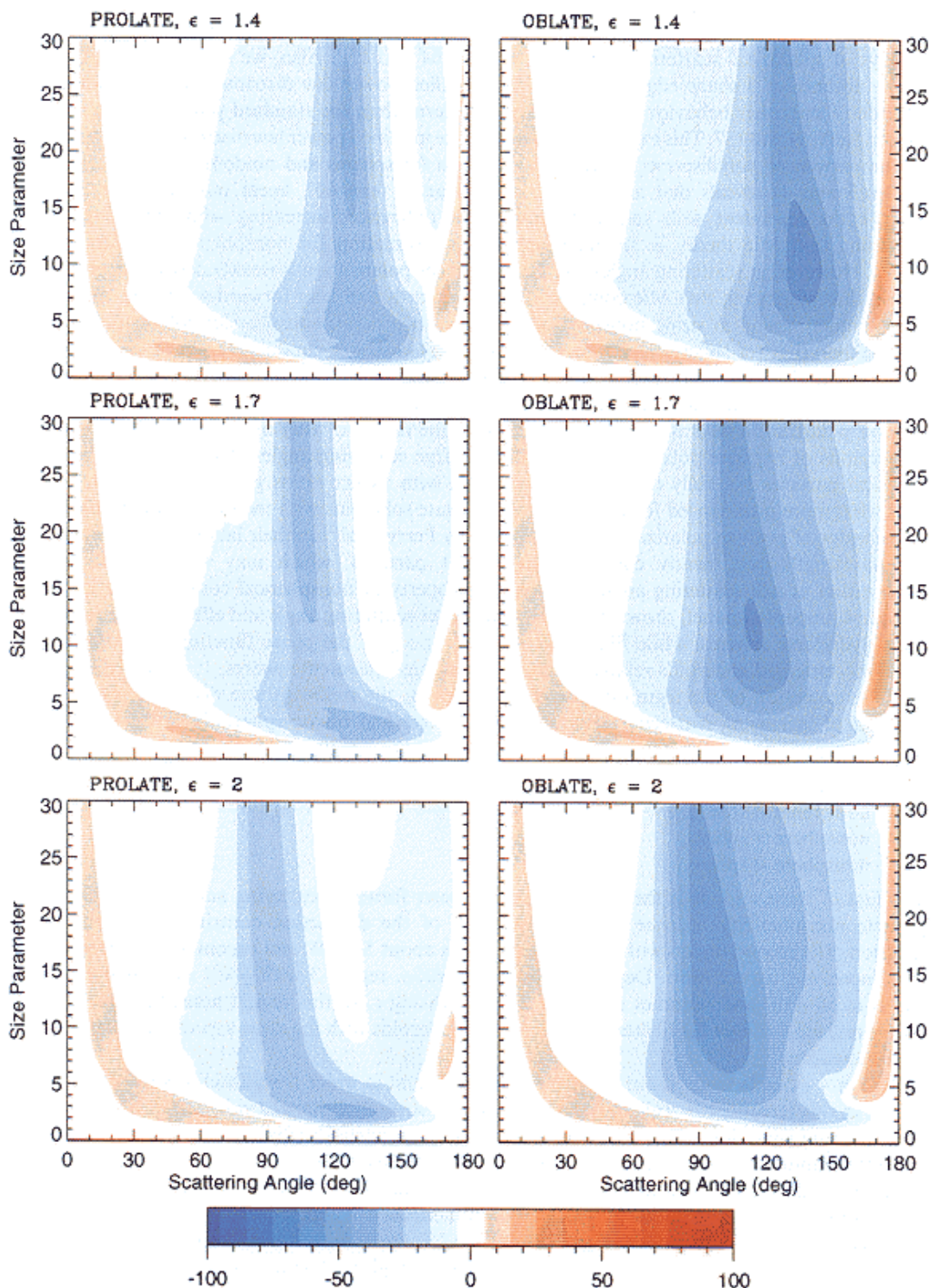


Plate 9. Ratio F_{34}/F_{11} in % vs scattering angle and effective size parameter for randomly oriented polydisperse spheroids.

variance is fixed at 0.1. For $v_{\text{eff}} = 0.1$, $x_1 \approx 0.8903 x_{\text{eff}}$ and $x_2 \approx 1.5654 x_{\text{eff}}$ so that the maximum monodisperse size parameter required in computations displayed in Plates 3–9 was close to 47. We note that this maximum effective size parameter is twice as large as that represented by recent surveys of spheroidal scattering published in Refs. 64 and 137. Also, we have found that, owing to the absence of a sharp edge at $x = x_1$, the modified power law distribution given by Eq. (91) provides a smoother behavior of the scattering patterns than the standard power law distribution used in Refs. 64 and 137. This explains the choice of the modified power law distribution for this study.

Comparison of polydisperse polarization diagrams for spheres and randomly oriented spheroids (Plates 3 and 4) reveals that at scattering angles larger than 60° , linear polarization is strongly aspect-ratio dependent with spherical-nonspherical differences increasing with increasing ϵ thus indicating that Mie theory is an inappropriate approximation for nonspherical particles in that region. However, at scattering angles less than 60° linear polarization is weakly dependent on particle shape, thus suggesting that Mie computations at forward- and near-forward-scattering angles may be potentially useful in sizing nonspherical particles. In general, nonspherical polarization is more neutral than that for spheres and shows less variability with size parameter and scattering angle. It is interesting, however, that the Rayleigh region extends to larger size parameters with increasing aspect ratio.^{64,130,141} The most prominent polarization feature of spheroidal scattering is the bridge of positive polarization near 120° which extends from the region of Rayleigh scattering and separates two regions of negative polarization at small and large scattering angles. This bridge is absent for spherical particles but fully develops for spheroids with aspect ratios greater than 1.6–1.7, being somewhat more pronounced for oblate than for prolate spheroids with the same ϵ . Interestingly, the same bridge of positive polarization was observed by Perry et al¹⁵¹ in their laboratory measurements for wavelength-sized, nearly cubically shaped salt particles, which may suggest that positive polarization at side-scattering angles is a typical property of nonspherical convex scattering.

Plate 4 (upper left panel) shows the phase function vs scattering angle and effective size parameter for polydisperse spheres, while Plate 5 shows the ratio ϱ of the phase function for polydisperse, randomly oriented spheroids relative to that for surface-equivalent spheres. It is clearly seen that, with the exception of the region of Rayleigh scattering, the following five distinct ϱ regions exist in order of increasing scattering angle for both prolate and oblate spheroids:^{137,144}

- (1) nonsphere \approx sphere,
- (2) nonsphere $>$ sphere,
- (3) nonsphere $<$ sphere,
- (4) nonsphere $>$ sphere,
- (5) nonsphere $<$ sphere.

The first of these regions is the region of nearly direct forward scattering and is least sensitive to particle nonsphericity because of the dominance of the diffraction contribution to the phase function. The second region with $\varrho > 1$ extends from about 5 to 30° and becomes more pronounced with increasing aspect ratio. Depending on aspect ratio, region 3 with $\varrho < 1$ extends from about 30–35 to 80–110° and becomes narrower with increasing ϵ . In this region nonspherical–spherical differences are stronger for oblate than for prolate spheroids with the same aspect ratio and increase with increasing ϵ .

Region 4 extends from about 80–110 to 150–160° and is wider for particles with larger aspect ratios. In this region ϱ can well exceed 4, indicating a strongly enhanced side-scattering as opposed to a deep and wide side-scattering minimum for spherical particles (Plate 4, upper left panel). Both the left boundary of this region and the position of maximum ϱ values shift towards smaller scattering angles with increasing ϵ . Interestingly, for prolate spheroids maximum ϱ values are larger for a moderate aspect ratio of 1.4 than for aspect ratios 1.7 and 2.

In region 5, ϱ can reach values smaller than 0.25, which means that another major effect of nonsphericity is to suppress the strong rainbow and glory features seen in calculations for surface-equivalent spheres (Plate 4, upper left panel). It should be noted however that the backscattering peak, usually associated with the glory, survives as a rise of the backscattered intensity at 180° relative to that at 170° .^{43,119,137,144} Furthermore, as shown in Fig. 5, oblate spheroids with aspect ratio 1.4 can have even larger phase function values at 180° than surface-equivalent spheres, causing values of ϱ greater than 1 and thereby generating an exception to the region 5

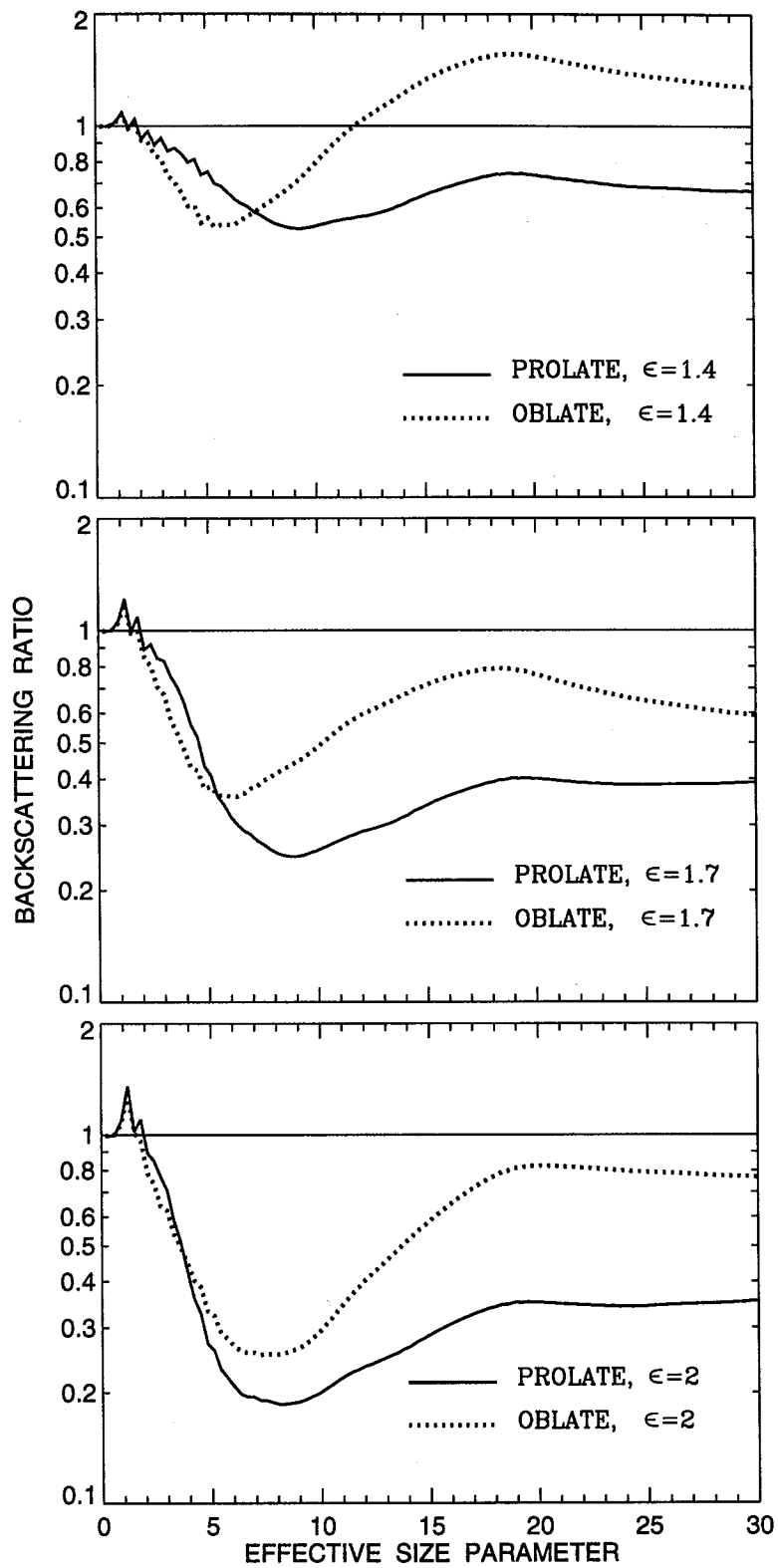


Fig. 5. Ratio of the phase function at $\Theta = 180^\circ$ for randomly oriented polydisperse spheroids relative to that for surface-equivalent spheres vs effective size parameter.

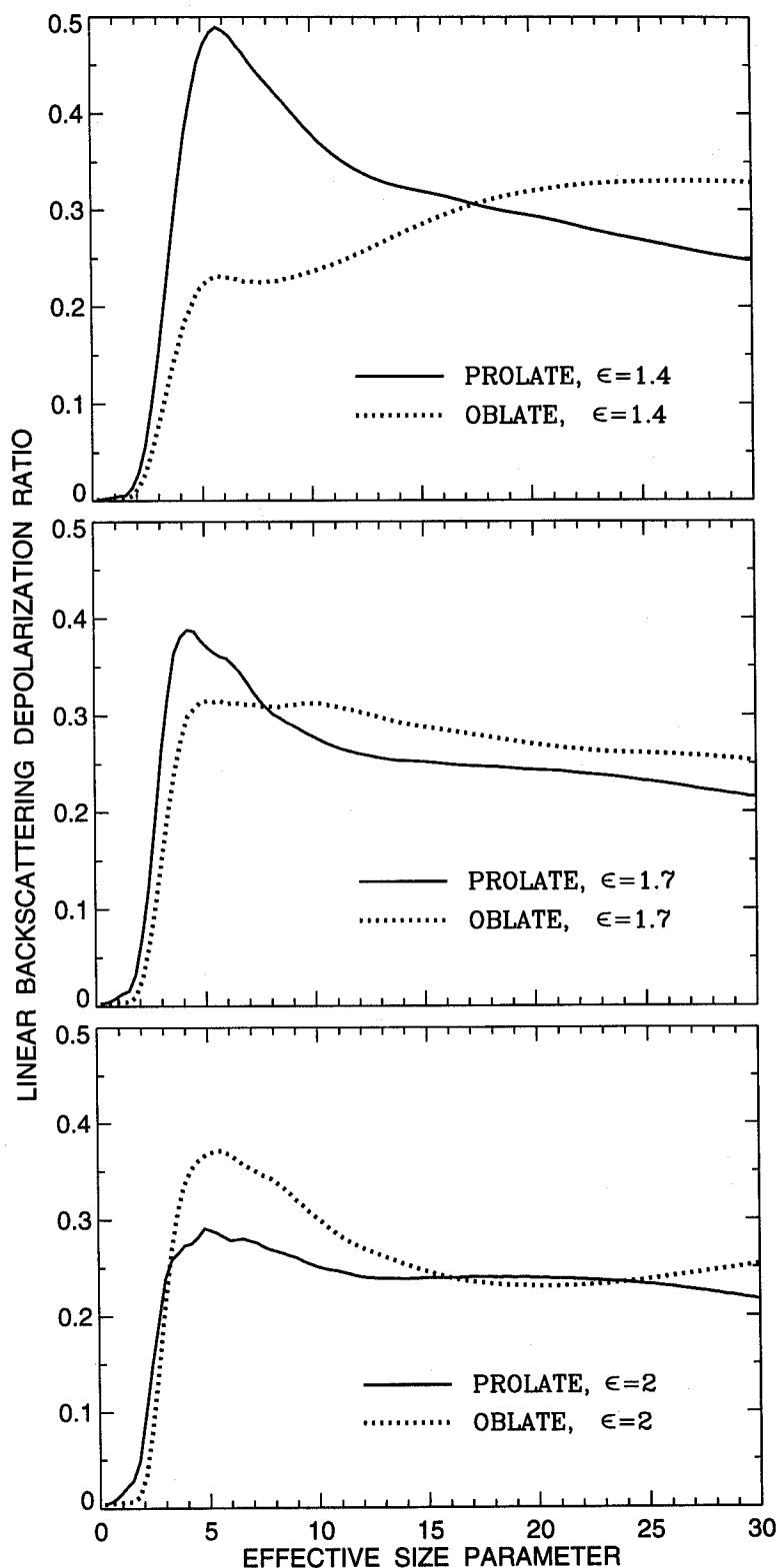


Fig. 6. Linear backscattering depolarization ratio vs effective size parameter for randomly oriented polydisperse spheroids.

criterion $\varrho < 1$. Figure 5 also shows that for most size parameters oblate spheroids have larger backscattering phase functions than prolate spheroids with the same aspect ratio and that the ratio of the nonspherical to spherical phase functions at $\Theta = 180^\circ$ has a distinct minimum at effective size parameters about 6–8. Interestingly, as Plate 5 demonstrates, at backscattering angles prolate–oblate differences are smaller for particles with $\epsilon = 1.7$ and 2 than for less-aspherical particles with $\epsilon = 1.4$. Also worth noting is that for prolate spheroids, region 5 becomes more pronounced with increasing aspect ratio, while for oblate spheroids ϱ can be smaller for $\epsilon = 1.7$ than for $\epsilon = 2$ at larger effective size parameters.

Although for spherical particles the ratio F_{22}/F_{11} is identically equal to 1, Plate 6 demonstrates that for spheroids it can significantly deviate from unity, especially at side- and backscattering angles. The angular dependence of F_{22}/F_{11} is quite different for prolate and oblate spheroids, making the ratio well suited for discriminating between elongated and flattened particles. For prolate spheroids, F_{22}/F_{11} has a pronounced minimum centered at $120\text{--}145^\circ$ which shifts towards smaller scattering angles with increasing aspect ratio. Another minimum occurs at backscattering angles, and surprisingly, is deeper for less-aspherical spheroids with $\epsilon = 1.4$ than for spheroids with $\epsilon = 1.7$ and 2. Oblate spheroids exhibit a minimum at around $150\text{--}170^\circ$, which becomes more pronounced for particles with $\epsilon = 2$, and a minimum at exactly the backscattering direction $\Theta = 180^\circ$ which exhibits a complicated dependence on the aspect ratio. Also, oblate spheroids with $\epsilon = 1.4$ show a shallow minimum at about $100\text{--}110^\circ$ which disappears with increasing aspect ratio. For both prolate and oblate spheroids, the ratio F_{22}/F_{11} at scattering angles less than 70° and in the region of Rayleigh scattering ($x_{\text{eff}} \lesssim 1$) is close to 1 and is practically insensitive to particle size and shape.

For spherical particles the ratio F_{33}/F_{11} is identically equal to the ratio F_{44}/F_{11} and is shown in Plate 4 (lower left panel). For spheroids these ratios can be substantially different, the ratio F_{44}/F_{11} being larger than F_{33}/F_{11} for most effective size parameters and scattering angles (Plates 7 and 8). For spheres, the ratio F_{33}/F_{11} (and thus F_{44}/F_{11}) has two negative regions at side- and backscattering angles separated by a narrow positive branch. With increasing aspect ratio, the side-scattering negative region shifts towards smaller scattering angles, weakens, and ultimately disappears, while the backscattering negative region becomes wider, especially for prolate spheroids. The backscattering region of negative F_{33}/F_{11} values is wider and deeper than that for F_{44}/F_{11} . Unlike the ratio F_{33}/F_{11} , the ratio F_{44}/F_{11} can be positive at exactly the backscattering direction. Both F_{33}/F_{11} and F_{44}/F_{11} are rather strongly size- and aspect-ratio-dependent and thus can be sensitive indicators of particle size and shape. In particular, the regions of negative F_{33}/F_{11} and F_{44}/F_{11} values are wider and deeper for prolate than for oblate spheroids with the same aspect ratio. The backscattering size parameter dependence of the ratio F_{44}/F_{11} is also rather different for prolate and oblate spheroids with the same ϵ .

Plates 4 (lower right panel) and 9 show that the general pattern of the sign of the ratio F_{34}/F_{11} is the same for spheres and spheroids with a broad side-scattering region of negative values separating two positive branches at small and large scattering angles. This result is in full agreement with laboratory measurements of Perry et al¹⁵¹ for wavelength-sized salt particles. The forward-scattering region is especially aspect-ratio-independent, which renders possible the use of Mie theory at small scattering angles for sizing nonspherical particles. However, large variations of the value of the ratio F_{34}/F_{11} with particle shape at side and backscattering angles make it sensitive to particle nonsphericity and appreciably different for prolate and oblate spheroids of the same aspect ratio. In particular, with increasing aspect ratio the region of smallest F_{34}/F_{11} -values becomes more shallow and shifts towards smaller scattering angles, while the backscattering positive branch becomes less pronounced. The region of negative values is more shallow and the backscattering positive branch is much weaker for prolate than for oblate spheroids. In general, the differences between prolate spheroids and spheres are larger than those between oblate spheroids and spheres.

Two quantities that are usually considered sensitive indicators of particle nonsphericity are the linear, δ_L , and circular, δ_C , backscattering depolarization ratios^{127,131,152–157} defined as

$$\delta_L = \frac{F_{11}(180^\circ) - F_{22}(180^\circ)}{F_{11}(180^\circ) + F_{22}(180^\circ)}, \quad (96)$$

$$\delta_C = \frac{F_{11}(180^\circ) + F_{44}(180^\circ)}{F_{11}(180^\circ) - F_{44}(180^\circ)}. \quad (97)$$

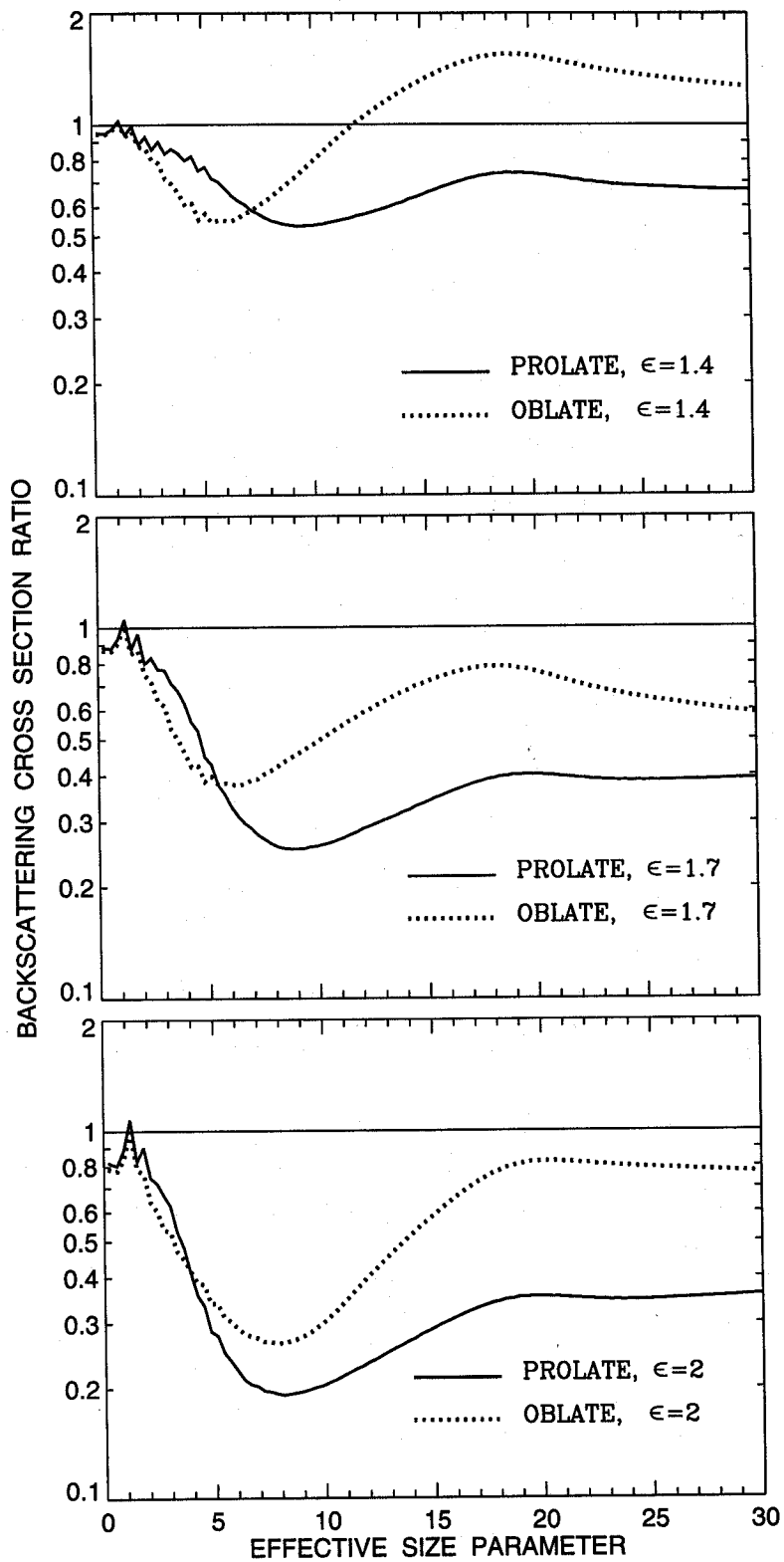


Fig. 7. Ratio of the backscattering cross section for randomly oriented polydisperse spheroids relative to that for surface-equivalent spheres vs effective size parameter.

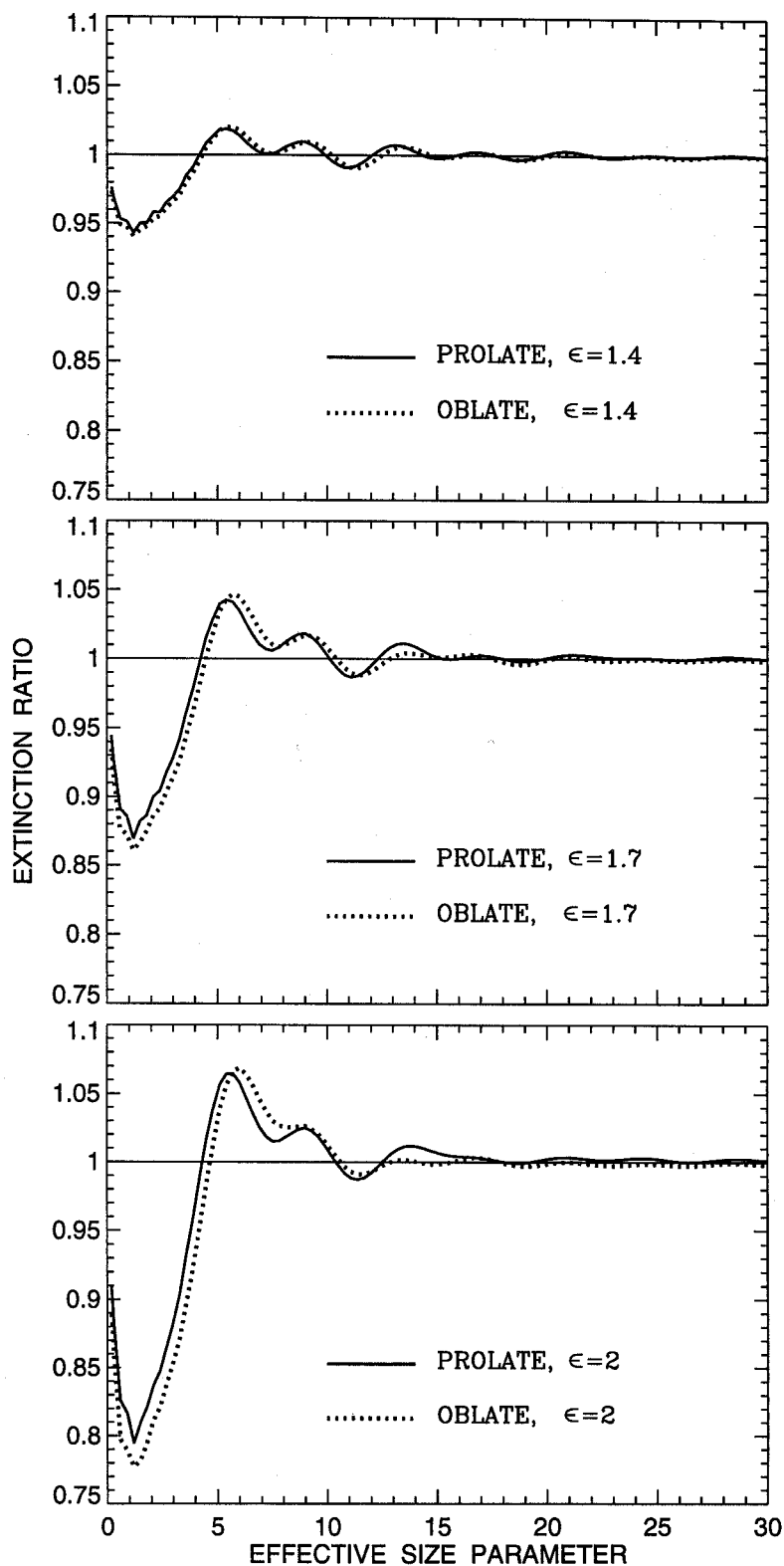


Fig. 8. Ratio of the extinction cross section for randomly oriented polydisperse spheroids relative to that for surface-equivalent spheres vs effective size parameter.

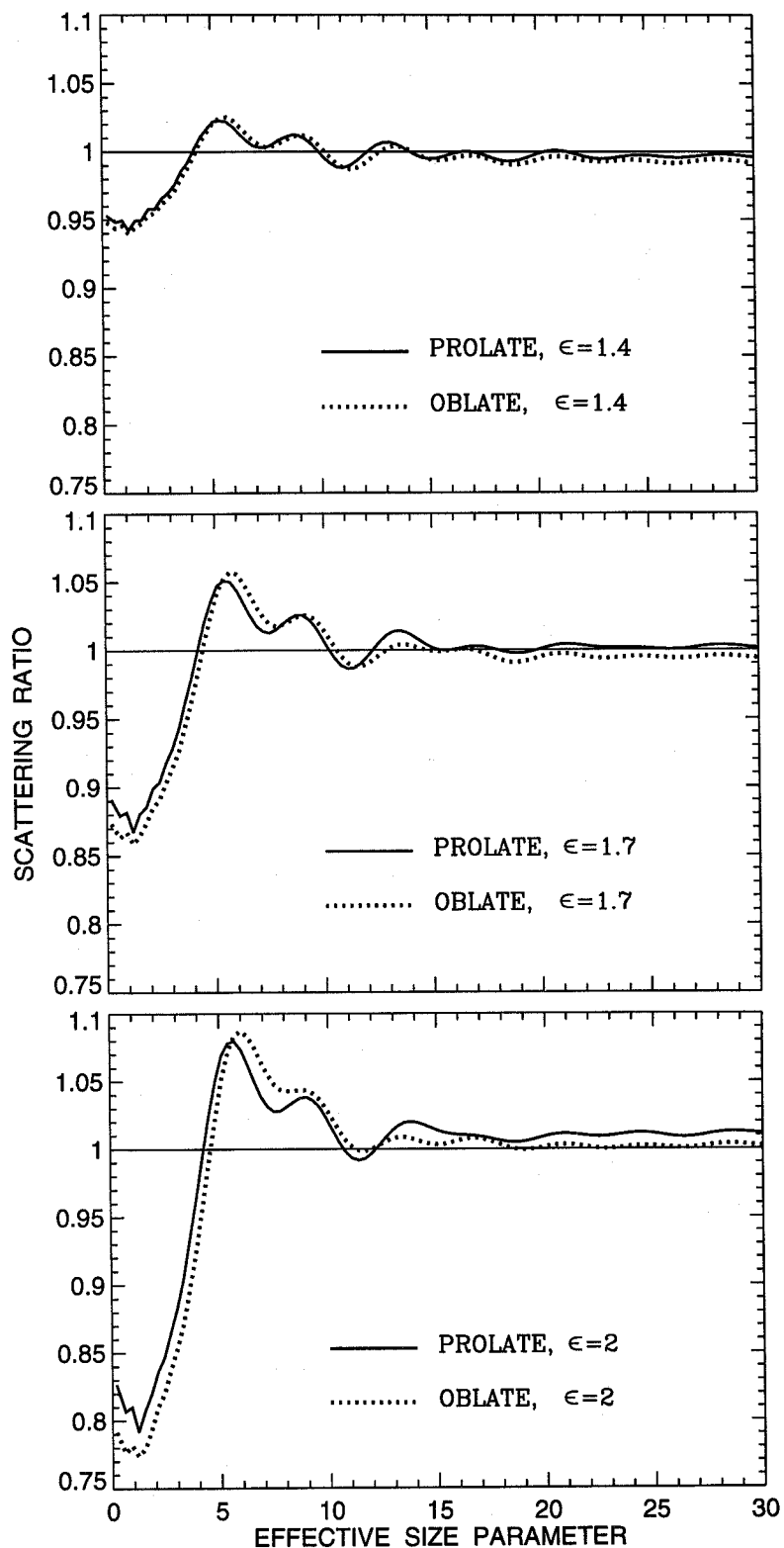


Fig. 9. Ratio of the scattering cross section for randomly oriented polydisperse spheroids relative to that for surface-equivalent spheres vs effective size parameter.

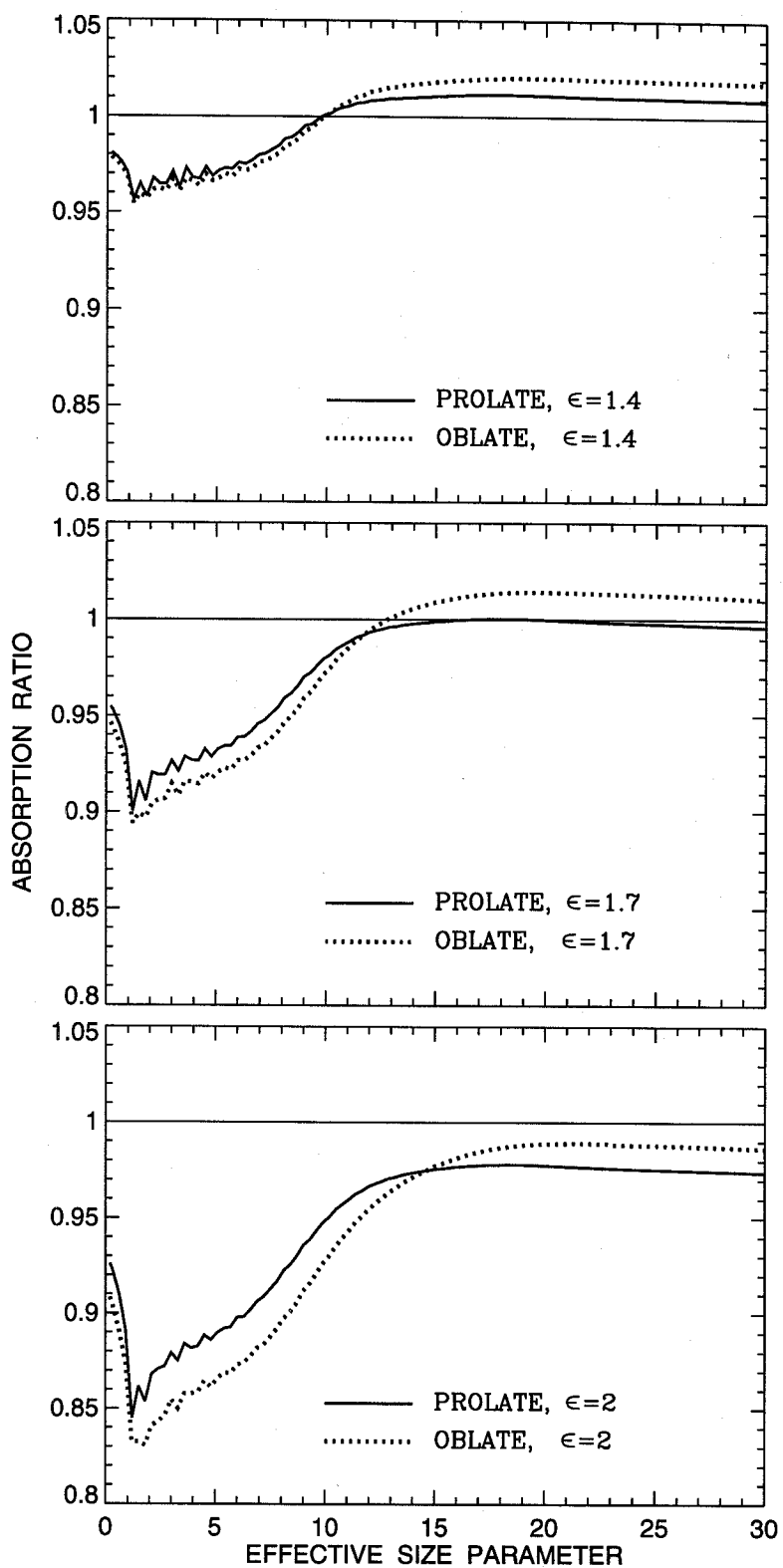


Fig. 10. Ratio of the absorption cross section for randomly oriented polydisperse spheroids relative to that for surface-equivalent spheres vs effective size parameter.

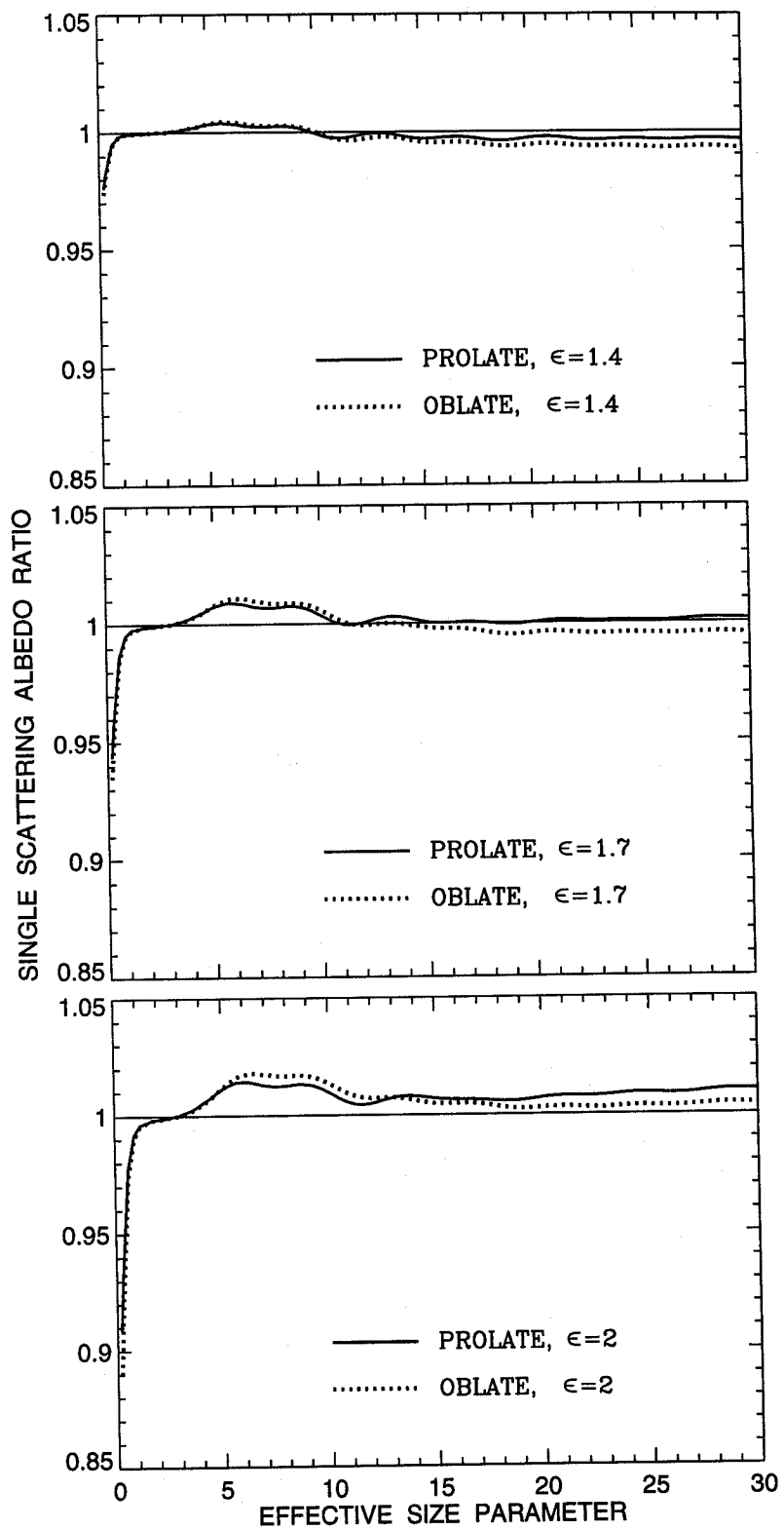


Fig. 11. Ratio of the single scattering albedo for randomly oriented polydisperse spheroids relative to that for surface-equivalent spheres vs effective size parameter.

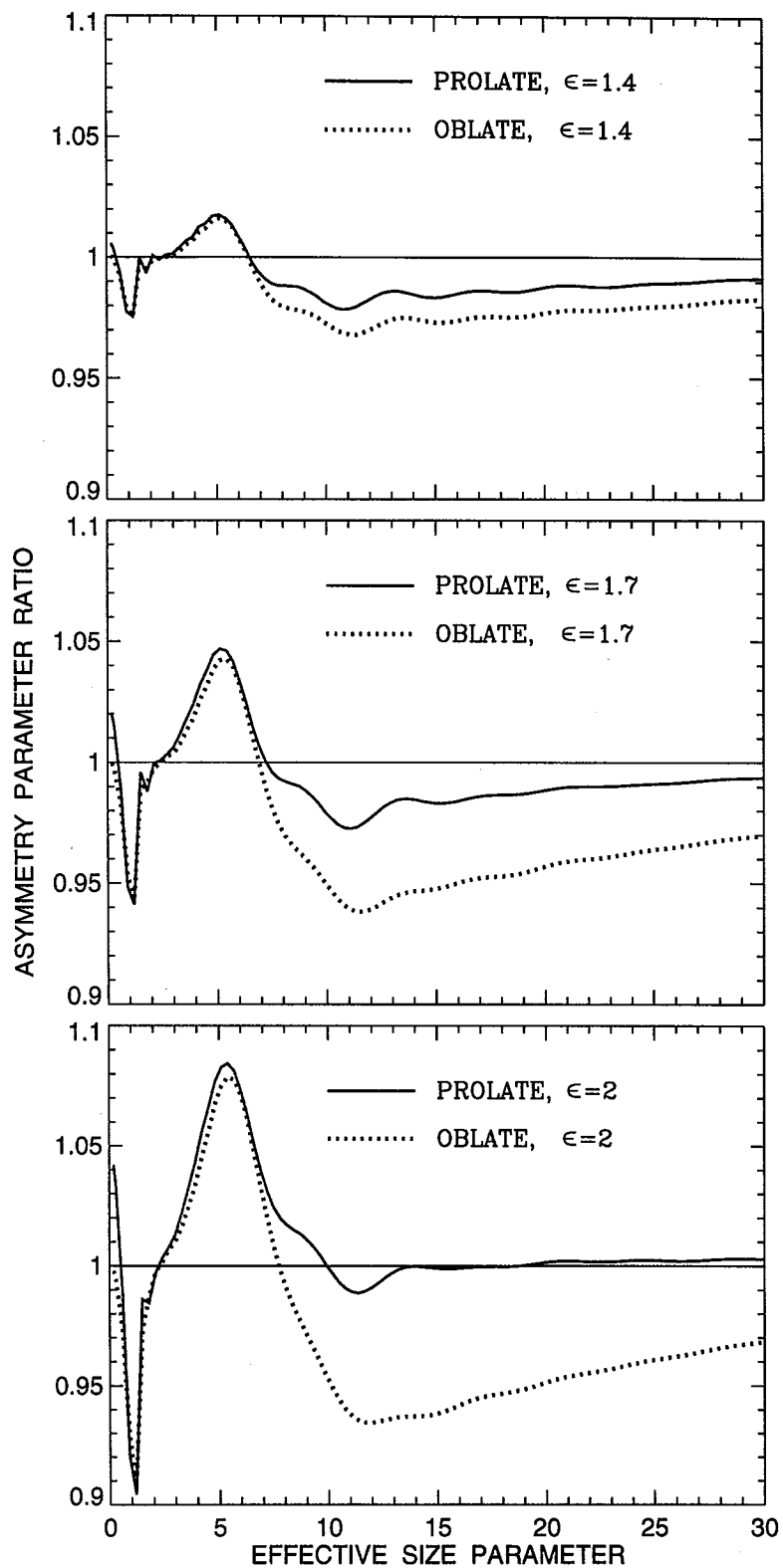


Fig. 12. Ratio of the asymmetry parameter of the phase function for randomly oriented polydisperse spheroids relative to that for surface-equivalent spheres vs effective size parameter.

For spheres both ratios vanish since $F_{22}(180^\circ) = F_{11}(180^\circ)$ and $F_{44}(180^\circ) = -F_{11}(180^\circ)$. For nonspherical particles these equalities do not generally hold, thus causing nonzero backscattering depolarization ratios. Figure 6 shows the linear backscattering depolarization ratio computed for randomly oriented polydisperse spheroids. The circular backscattering depolarization ratio can be calculated using the relationship¹³⁹

$$\delta_C = \frac{2\delta_L}{1 - \delta_L}. \quad (98)$$

It is seen that for both prolate and oblate spheroids δ_L can substantially deviate from zero thus illustrating its use as an indicator of nonsphericity. However, the backscattering depolarization ratios cannot be considered unambiguous indicators of the degree of the departure of particle shape from that of a sphere. Indeed, the maximum δ_L value for prolate spheroids with $\epsilon = 1.4$ is larger than that for $\epsilon = 1.7$ and 2. Furthermore, computations reported in Ref. 139 show that even larger δ_L values can be found for aspect ratios as small as 1.05–1.1. As Fig. 6 demonstrates (see also Plate 1 of Ref. 139), large depolarization values can be reached at size parameters smaller than 6, i.e., for particles smaller than the wavelength. At these small size parameters the traditional geometric optics concepts of rays, refractions, and reflections are inapplicable.¹ Moreover, the geometric optics completely fails to explain the strong and complicated size-parameter dependence of the depolarization ratios as demonstrated by Plate 1 of Ref. 139 and Fig. 4 of Ref. 112. Therefore, our results indicate that multiple internal reflections, as suggested in Refs. 158 and 159, cannot be the universal explanation of backscattering depolarization for nonspherical particles.

Another important backscattering characteristic widely used in lidar applications^{160,161} is the so-called backscattering cross section defined as the product $C_{\text{sca}} F_{11}(180^\circ)$, where C_{sca} is the scattering cross section. Figure 7 shows the ratio of the backscattering cross section for randomly oriented polydisperse spheroids relative to that for surface-equivalent spheres. Not surprisingly, this figure differs from Fig. 5 only at small size parameters where the ratio of the scattering cross sections for nonspherical and surface-equivalent spherical particles noticeably deviates from 1 (see below). It is seen that nonspherical–spherical differences in the backscattering cross section are significant, thus suggesting that the effect of particle shape should be explicitly taken into account in analyzing backscattering measurements for nonspherical particles. This conclusion is in agreement with the result of Ref. 161 based on the analysis of lidar measurements of Saharan dust aerosols. In general, spheroids are weaker backscatterers than surface-equivalent spheres, especially at size parameters from about 5 to 15. However, oblate spheroids with aspect ratio 1.4 show that suppressed scattering at $\Theta = 180^\circ$ is not the universal characteristic of nonspherical particles.

Unlike the elements of the scattering matrix, the integral photometric characteristics (extinction, scattering, and absorption cross sections, single scattering albedo, and asymmetry parameter of the phase function) are much less dependent on particle shape, as Figs. 8–12 show. We note that maximum nonspherical–spherical differences are observed at effective size parameters smaller than about 15. For the optical cross sections and single scattering albedo the differences are maximum at especially small effective size parameters and may be an artifact of comparing surface-equivalent rather than volume-equivalent particles.¹³⁷ Interestingly, the asymptotic geometric optics limit of one for the extinction cross section ratio is reached at relatively small size parameters of about 15. Nonspherical–spherical differences are especially small for the single scattering albedo at size parameters exceeding 2. The curves for prolate and oblate spheroids with the same aspect ratio are very close to one another except for the asymmetry parameter of the phase function where prolate–oblate differences can be much larger than prolate–spherical differences.

Acknowledgements—We thank N. V. Voshchinnikov for providing us with his code based on the separation of variables method for spheroids and described in Ref. 23. We are grateful to J. W. Hovenier, K. Lumme, and H. C. van de Hulst for careful reading of the manuscript and valuable comments and to N. T. Zakharova for help with graphics. M. I. Mishchenko and L. D. Travis acknowledge support from the Earth Observing System Project managed by Goddard Space Flight Center in providing for the Earth Observing Scanning Polarimeter instrument and algorithm development, the NASA Office of Mission to Planet Earth, and the NASA FIRE III Project. D. W. Mackowski acknowledges support from the DuPoint Educational Aid Grant Program.

Note added in proof—This review would be incomplete without mentioning recent publications (Refs. 162–171) in which the (superposition) T -matrix method has been further developed and/or used for practical applications.

REFERENCES

1. H. C. van de Hulst, *Light Scattering by Small Particles*, Wiley, New York, NY (1957).
2. C. F. Bohren and D. R. Huffman, *Absorption and Scattering of Light by Small Particles*, Wiley, New York, NY (1983).
3. J. E. Hansen and L. D. Travis, *Space Sci. Rev.* **16**, 527 (1974).
4. D. W. Schuerman (ed.), *Light Scattering by Irregularly Shaped Particles*, Plenum Press, New York, NY (1980).
5. V. K. Varadan and V. V. Varadan (eds.), *Acoustic, Electromagnetic and Elastic Wave Scattering—Focus on the T-matrix Approach*, Pergamon Press, New York, NY (1980).
6. T. Oguchi, *Radio Sci.* **16**, 691 (1981).
7. A. R. Holt, *Radio Sci.* **17**, 929 (1982).
8. J. P. Mon, *Radio Sci.* **17**, 953 (1982).
9. P. W. Barber and H. Massoudi, *Aerosol Sci. Technol.* **1**, 303 (1982).
10. C. F. Bohren and S. B. Singham, *J. Geophys. Res.* **96**, 5269 (1991).
11. W. J. Wiscombe and A. Mugnai, NASA Ref. Publ. 1157, NASA/GSFC, Greenbelt, MD (1986).
12. P. C. Waterman, *Proc. IEEE* **53**, 805 (1965).
13. P. C. Waterman, *Alta Frequenza (Speciale)* **38**, 348 (1969).
14. P. C. Waterman, *Phys. Rev. D* **3**, 825 (1971).
15. P. C. Waterman, *J. Appl. Phys.* **50**, 4550 (1979).
16. P. C. Waterman and N. E. Pedersen, *J. Appl. Phys.* **59**, 2609 (1986).
17. L. Tsang, J. A. Kong, and R. T. Shin, *Theory of Microwave Remote Sensing*, Wiley, New York, NY (1985).
18. V. V. Varadan, A. Lakhtakia, and V. K. Varadan, *J. Acoust. Soc. Am.* **84**, 2280 (1988).
19. J. I. Hage, J. M. Greenberg, and R. T. Wang, *Appl. Opt.* **30**, 1141 (1991).
20. B. T. Draine and P. J. Flatau, *JOSA A* **11**, 1491 (1994).
21. K. Lumme and J. Rahola, *Astrophys. J.* **425**, 653 (1994).
22. S. Asano and M. Sato, *Appl. Opt.* **19**, 962 (1980).
23. N. V. Voshchinnikov and V. G. Farafonov, *Astrophys. Space Sci.* **204**, 19 (1993).
24. M. I. Mishchenko, *JOSA A* **8**, 871 (1991); errata, *ibid.* **9**, 497 (1992).
25. D. A. Varshalovich, A. N. Moskalev, and V. K. Khersonskii, *Quantum Theory of Angular Momentum*, World Scientific, Singapore (1988).
26. V. K. Varadan, in *Acoustic, Electromagnetic and Elastic Wave Scattering—Focus on the T-Matrix Approach*, V. K. Varadan and V. V. Varadan, eds., pp. 103–134, Pergamon Press, New York, NY (1980); V. V. Varadan and V. K. Varadan, *Phys. Rev. D* **21**, 388 (1980).
27. D. S. Saxon, *Phys. Rev.* **100**, 1771 (1955).
28. S. Ström, in *Field Representations and Introduction to Scattering*, V. V. Varadan, A. Lakhtakia, and V. K. Varadan, eds., pp. 143–164, North-Holland, Amsterdam (1991).
29. M. I. Mishchenko, *Kinem. Fiz. Nebes. Tel* **7**(5), 93 (1991).
30. L. E. Paramonov, *JOSA A* **12**, 2698 (1995).
31. M. I. Mishchenko, *Astrophys. Space Sci.* **164**, 1 (1990).
32. F. Borghese, P. Denti, R. Saija, G. Toscano, and O. I. Sindoni, *Aerosol Sci. Technol.* **3**, 227 (1984).
33. N. G. Khlebtsov, *Appl. Opt.* **31**, 5359 (1992).
34. J. W. Hovenier and C. V. M. van der Mee, *Astron. Astrophys.* **128**, 1 (1983).
35. J. F. de Haan, P. B. Bosma, and J. W. Hovenier, *Astron. Astrophys.* **183**, 371 (1987).
36. C. V. M. van der Mee and J. W. Hovenier, *Astron. Astrophys.* **228**, 559 (1990).
37. I. M. Gelfand, R. A. Minlos, and Z. Ya. Shapiro, *Representations of the Rotation and Lorentz Groups and Their Applications*, Pergamon Press, Oxford (1963).
38. S. Chandrasekhar, *Radiative Transfer*, Oxford Univ. Press, London (1950).
39. V. V. Sobolev, *Light Scattering in Planetary Atmospheres*, Pergamon Press, Oxford (1975).
40. H. C. van de Hulst, *Multiple Light Scattering*, Academic Press, New York, NY (1980).
41. H. Domke, *Astrophys. Space Sci.* **29**, 379 (1974).
42. C. E. Siewert, *Astrophys. J.* **245**, 1080 (1981).
43. M. I. Mishchenko, *Appl. Opt.* **32**, 4652 (1993).
44. W. M. F. Wauben, private communication (1993).
45. E. Fucile, F. Borghese, P. Denti, and R. Saija, *JOSA A* **10**, 2611 (1993).
46. M. I. Mishchenko, *Astrophys. J.* **367**, 561 (1991).
47. M. I. Mishchenko, *J. Electromagn. Waves Appl.* **6**, 1341 (1992).
48. E. Fucile, F. Borghese, P. Denti, and R. Saija, *Appl. Opt.* **34**, 4552 (1995).
49. J. Vivekanandan, W. M. Adams, and V. N. Bringi, *J. Appl. Meteorol.* **30**, 1053 (1991).
50. P. M. Morse and H. Feshbach, *Methods of Theoretical Physics*, McGraw-Hill, New York, NY (1953).
51. P. Barber and C. Yeh, *Appl. Opt.* **14**, 2864 (1975).
52. S. Ström and W. Zheng, *Radio Sci.* **22**, 1273 (1987).
53. P. W. Barber and S. C. Hill, *Light Scattering by Particles: Computational Methods*, World Scientific, Singapore (1990).
54. A. Boström, G. Kristensson, and S. Ström, in *Field Representations and Introduction to Scattering*, V. V. Varadan, A. Lakhtakia, and V. K. Varadan, eds., pp. 165–210, North-Holland, Amsterdam (1991).

55. S. Ström, *Am. J. Phys.* **43**, 1060 (1975).
56. J. B. Schneider and I. C. Peden, *IEEE Trans. Antennas Propag.* **36**, 1317 (1988).
57. J. Schneider, J. Brew, and I. C. Peden, *IEEE Trans. Geosci. Remote Sens.* **29**, 555 (1991).
58. B. Peterson and S. Ström, *Phys. Rev. D* **10**, 2670 (1974).
59. V. N. Bringi and T. A. Seliga, *Ann. Telecommun.* **32**, 392 (1977).
60. D.-S. Wang and P. W. Barber, *Appl. Opt.* **18**, 1190 (1979).
61. D.-S. Wang, H. C. H. Chen, P. W. Barber, and P. J. Wyatt, *Appl. Opt.* **18**, 2672 (1979).
62. A. Lakhtakia, V. K. Varadan, and V. V. Varadan, *Appl. Opt.* **24**, 4146 (1985).
63. F. Kuik, Ph.D. thesis, Free Univ., Amsterdam (1992).
64. M. I. Mishchenko and L. D. Travis, *JQSRT* **51**, 759 (1994).
65. M. I. Mishchenko, *JQSRT* **46**, 171 (1991).
66. F. Kuik, J. F. de Haan, and J. W. Hovenier, *JQSRT* **47**, 477 (1992).
67. W. H. Press, S. A. Teukolsky, W. T. Vetterling, and B. P. Flannery, *Numerical Recipes*, Cambridge Univ. Press, Cambridge (1992).
68. P. W. Barber, *IEEE Trans. Microwave Theory Tech.* **25**, 373 (1977).
69. M. F. Iskander, A. Lakhtakia, and C. H. Durney, *IEEE Trans. Antennas Propag.* **31**, 317 (1983).
70. A. Lakhtakia, M. F. Iskander, and C. H. Durney, *IEEE Trans. Microwave Theory Tech.* **31**, 640 (1983).
71. M. F. Iskander and A. Lakhtakia, *Appl. Opt.* **23**, 948 (1984).
72. A. Lakhtakia and M. F. Iskander, *IEEE Trans. Electromagn. Compat.* **25**, 448 (1983).
73. M. F. Iskander, S. C. Olson, R. E. Benner, and D. Yoshida, *Appl. Opt.* **25**, 2514 (1986).
74. M. F. Iskander, H. Y. Chen, and T. V. Duong, *IEEE Trans. Electromagn. Compat.* **31**, 157 (1989).
75. P. C. Waterman, in *Computer Techniques for Electromagnetics*, Vol. 7, R. Mittra, ed., pp. 97–157, Pergamon Press, Oxford (1973).
76. A. Lakhtakia, V. K. Varadan, and V. V. Varadan, *Appl. Opt.* **23**, 3502 (1984).
77. A. Lakhtakia, V. V. Varadan, and V. K. Varadan, *J. Appl. Phys.* **58**, 4525 (1985).
78. M. I. Mishchenko and L. D. Travis, *Opt. Comm.* **109**, 16 (1994).
79. S. G. Warren, *Appl. Opt.* **23**, 1206 (1984).
80. A. Macke, M. I. Mishchenko, K. Muinonen, and B. E. Carlson, *Opt. Lett.* **20**, 1934 (1995).
81. Y. Takano and M. Tanaka, *Appl. Opt.* **19**, 2781 (1980).
82. C. Liang and Y. T. Lo, *Radio Sci.* **2**, 1481 (1967).
83. J. H. Bruning and Y. T. Lo, *IEEE Trans. Antennas Propag.* **19**, 378 (1971); *ibid.* **19**, 391 (1971).
84. B. Peterson and S. Ström, *Phys. Rev. D* **8**, 3661 (1973).
85. B. Peterson, *Phys. Rev. A* **16**, 1363 (1977).
86. O. R. Cruzan, *Q. Appl. Math.* **20**, 33 (1962).
87. K. A. Fuller, Ph.D. thesis, Texas A&M Univ., College Station, TX (1987).
88. K. A. Fuller and G. W. Kattawar, *Opt. Lett.* **13**, 90 (1988); *ibid.* **13**, 1063 (1988).
89. F. Borghese, P. Denti, R. Saija, and O. I. Sindoni, *J. Aerosol. Sci.* **20**, 1079 (1989).
90. K. A. Fuller, *Appl. Opt.* **30**, 4716 (1991).
91. D. W. Mackowski, *Proc. R. Soc. London A* **433**, 599 (1991).
92. A.-K. Hamid, I. R. Ceric, and M. Hamid, *Can. J. Phys.* **68**, 1419 (1990); *IEE Proc. H* **138**, 565 (1991).
93. W. C. Chew, Y. M. Wang, and L. Gürel, *J. Electromagn. Waves Appl.* **6**, 1537 (1992).
94. Y. M. Wang and W. C. Chew, *IEEE Trans. Antennas Propag.* **41**, 1633 (1993).
95. W. C. Chew, C. C. Lu, and Y. M. Wang, *JOSA A* **11**, 1528 (1994).
96. D. W. Mackowski, *JOSA A* **11**, 2851 (1994).
97. K. A. Fuller, *JOSA A* **11**, 3251 (1994).
98. L. F. Fonseca, M. Gomez, and L. Cruz, *Physica A* **207**, 123 (1994).
99. Y. C. Tzeng and A. K. Fung, *J. Electromagn. Waves Appl.* **8**, 61 (1994).
100. C. C. Lu, W. C. Chew, and L. Tsang, *Radio Sci.* **30**, 25 (1995).
101. K. A. Fuller, *JOSA A* **12**, 881 (1995).
102. F. de Daran, V. Vignéras-Lefebvre, and J. P. Parneix, *IEEE Trans. Magn.* **31**, 1598 (1995).
103. Y.-L. Xu, *Appl. Opt.* **34**, 4573 (1995).
104. L. M. Zurk, L. Tsang, K. H. Ding, and D. P. Winebrenner, *JOSA A* **12**, 1772 (1995).
105. M. P. Ioannidou, N. C. Skaropoulos, and D. P. Chrissoulidis, *JOSA A* **12**, 1782 (1995).
106. L. M. Zurk, L. Tsang, and D. P. Winebrenner, *Radio Sci.*, submitted (1996).
107. F. Borghese, P. Denti, R. Saija, and O. I. Sindoni, *JOSA A* **9**, 1327 (1992).
108. F. Borghese, P. Denti, and R. Saija, *Appl. Opt.* **33**, 484 (1994); errata, *ibid.* **34**, 5556 (1995).
109. K. A. Fuller, *JOSA A* **12**, 893 (1995).
110. G. Videen, D. Ngo, P. Chýlek, and R. G. Pinnick, *JOSA A* **12**, 922 (1995).
111. M. I. Mishchenko and D. W. Mackowski, *Opt. Lett.* **19**, 1604 (1994).
112. M. I. Mishchenko, D. W. Mackowski, and L. D. Travis, *Appl. Opt.* **34**, 4589 (1995).
113. S. Ström and W. Zheng, *IEEE Trans. Antennas Propag.* **36**, 376 (1988).
114. W. Zheng, *IEEE Trans. Antennas Propag.* **36**, 1396 (1988).
115. W. Zheng and S. Ström, *IEEE Trans. Antennas Propag.* **37**, 373 (1989).
116. C. Warner and A. Hizal, *Radio Sci.* **11**, 921 (1976).
117. M. F. Iskander, P. W. Barber, C. H. Durney, and H. Massoudi, *IEEE Trans. Microwave Theory Tech.* **28**, 801 (1980).

118. P. W. Barber, D.-S. Wang, and M. B. Long, *Appl. Opt.* **20**, 1121 (1981).
119. S. C. Hill, A. C. Hill, and P. W. Barber, *Appl. Opt.* **23**, 1025 (1984).
120. K. Aydin and T. A. Seliga, *J. Atmos. Sci.* **41**, 1887 (1984).
121. P. E. Geller, T. G. Tsuei, and P. W. Barber, *Appl. Opt.* **24**, 2391 (1985).
122. C. D. Kummerov and J. A. Weinman, *IEEE Trans. Geosci. Remote Sens.* **26**, 629 (1988).
123. H. H. Barksdale and C. W. Bostian, *IEEE Trans. Antennas Propag.* **36**, 1033 (1988).
124. V. N. Lopatin and F. Ya. Sid'ko, *Introduction to Optics of Cell Suspensions*, Nauka, Novosibirsk (1988) (in Russian).
125. M. Hofer and O. Glatter, *Appl. Opt.* **28**, 2389 (1989).
126. F. Ya. Sid'ko, V. N. Lopatin, and L. E. Paramonov, *Polarization Characteristics of Suspensions of Biological Particles*, Nauka, Novosibirsk (1990) (in Russian).
127. O. B. Toon, E. V. Browell, S. Kinne, and J. Jordan, *Geophys. Res. Lett.* **17**, 393 (1990).
128. N. G. Khlebtsov, A. G. Melnikov, and V. A. Bogatyrev, *J. Colloid Interface Sci.* **146**, 463 (1991).
129. M. I. Mishchenko, *Earth Moon Planets* **53**, 149 (1991); M. I. Mishchenko, *Astrophys. Space Sci.* **180**, 163 (1991).
130. M. I. Mishchenko, *Earth Moon Planets* **57**, 203 (1992).
131. C. Flesia, L. de Schoulepenikoff, A. Mugnai, and L. Stefanutti, in *IRS'92: Current Problems in Atmospheric Radiation*, S. Keevallik and O. Kärner, eds., pp. 96–100, Deepak, Hampton, VA (1993); C. Flesia, A. Mugnai, Y. Eemery, S. Godin, L. de Schoulepenikoff, and V. Mitev, *Geophys. Res. Lett.* **21**, 1443 (1994).
132. Z. Xing, Ph.D. thesis, Leiden Univ. (1993); Z. Xing and J. M. Greenberg, *JOSA A* **11**, 657 (1994).
133. M. I. Mishchenko, *JQSRT* **52**, 95 (1994).
134. K. C. Ho and F. S. Allen, *Inv. Probl.* **10**, 387 (1994).
135. L. E. Paramonov, *Opt. Atmos. Okeana* **7**, 1139 (1994); *Opt. Spektrosk.* **77**, 660 (1994).
136. A. Q. Sierra and A. V. Delgado Mora, *Appl. Opt.* **34**, 6256 (1995).
137. M. I. Mishchenko and L. D. Travis, *Appl. Opt.* **33**, 7206 (1994).
138. M. I. Mishchenko, A. A. Lacis, B. E. Carlson, and L. D. Travis, *Geophys. Res. Lett.* **22**, 1077 (1995).
139. M. I. Mishchenko and J. W. Hovenier, *Opt. Lett.* **20**, 1356 (1995).
140. R. Ruppin, *J. Phys. D* **23**, 757 (1990).
141. F. Kuik, J. F. de Haan, and J. W. Hovenier, *Appl. Opt.* **33**, 4906 (1994).
142. A. Mugnai and W. J. Wiscombe, *J. Atmos. Sci.* **37**, 1291 (1980).
143. A. Mugnai and W. J. Wiscombe, *Appl. Opt.* **25**, 1235 (1986).
144. W. J. Wiscombe and A. Mugnai, *Appl. Opt.* **27**, 2405 (1988).
145. A. Mugnai and W. J. Wiscombe, *Appl. Opt.* **28**, 3061 (1989).
146. P. Chylek, V. Ramaswamy, R. Cheng, and R. G. Pinnick, *Appl. Opt.* **20**, 2980 (1981).
147. M. I. Mishchenko and D. W. Mackowski, *JQSRT* **55**, 683 (1996).
148. G. A. d'Almeida, P. Koepke, and E. P. Shettle, *Atmospheric Aerosols*, Deepak, Hampton, VA (1991).
149. J. F. de Haan, Ph.D. thesis, Free Univ., Amsterdam (1987).
150. P. Stammes, Ph.D. thesis, Free Univ., Amsterdam (1989).
151. R. J. Perry, A. J. Hunt, and D. R. Huffman, *Appl. Opt.* **17**, 2700 (1978).
152. K. Sassen, *Bull. Am. Meteorol. Soc.* **72**, 1848 (1991).
153. W. L. Eberhard, *Appl. Opt.* **31**, 6485 (1992).
154. S. J. Ostro, *Rev. Mod. Phys.* **65**, 1235 (1993).
155. G. L. Stephens, *Remote Sensing of the Lower Atmosphere*, Oxford Univ. Press, New York, NY (1994).
156. E. Rignot, *J. Geophys. Res.* **100**, 9389 (1995).
157. C. Tang and K. Aydin, *IEEE Trans. Geosci. Remote Sens.* **33**, 93 (1995).
158. K.-N. Liou and H. Lahore, *J. Appl. Meteorol.* **13**, 257 (1974).
159. R. H. Zerull, *Beitr. Phys. Atmos.* **49**, 168 (1976).
160. G. S. Kent, G. K. Yue, U. O. Farrukh, and A. Deepak, *Appl. Opt.* **22**, 1655 (1983); J. D. Klett, *ibid.* **24**, 1638 (1985); V. Srivastava, M. A. Jarzembski, and D. A. Bowdle, *ibid.* **31**, 1904 (1992).
161. Y. Sasano and E. V. Browell, *Appl. Opt.* **28**, 1670 (1989).
162. S. T. Massie, P. L. Bailey, J. C. Gille, E. C. Lee, J. L. Mergenthaler, A. E. Roche, J. B. Kumer, E. F. Fishbein, J. W. Waters, and W. A. Lahoz, *J. Atmos. Sci.* **51**, 3027 (1994).
163. N. G. Khlebtsov, V. A. Bogatyrev, L. A. Dykman, and A. G. Melnikov, *Colloid. J.* **57**, 384 (1995).
164. P. Chylek, G. Videen, D. Ngo, R. G. Pinnick, and J. D. Klett, *J. Geophys. Res.* **100**, 16325 (1995).
165. D. W. Mackowski and P. D. Jones, *J. Thermophys. Heat Transfer* **9**, 193 (1995).
166. W. C. Chew and C. C. Lu, *IEEE Trans. Antennas Propag.* **43**, 1483 (1995).
167. J. Haferman, Ph.D. thesis, Univ. of Iowa, Iowa City, IA (1995).
168. J. W. Hovenier, K. Lumme, M. I. Mishchenko, N. V. Voschinnikov, D. W. Mackowski, and J. Rahola, *JQSRT* in press (1996).
169. M. I. Mishchenko, L. D. Travis, and A. Macke, *Appl. Opt.* **35**, 4927 (1996).
170. M. I. Mishchenko, *Opt. Lett.* **21**, 623 (1996).
171. S. Liang and M. I. Mishchenko, *Remote Sens. Environ.* **60**, 163 (1997).